Constrained Thrust Allocation for Underwater Vehicles Using a DH-Based Newton-Euler Model and ADMM

Bhushan Thool, Jagadeesh Kadiyam, and Santakumar Mohan

Abstract Accurate dynamic modeling and efficient thrust allocation are essential for controlling over-actuated underwater vehicles. Many existing allocation methods rely on Euler-angle-based NewtonEuler formulations, which become complex for modular or multibody systems and scale poorly when hydrodynamic effects and actuator constraints are considered. This paper presents a thrust allocation framework based on a Denavit-Hartenberg (DH) parameter-driven NewtonEuler dynamic model, using virtual reference frames to provide a modular, computationally efficient representation without Euler-angle singularities. Thrust allocation is formulated as a constrained quadratic programming problem incorporating rigid-body dynamics, added mass, hydrodynamic damping, restoring forces, and actuator saturation. An alternating direction method of multipliers(ADMM)-based solution enables real-time implementation and improves trajectory tracking and energy efficiency compared with pseudoinverse allocation.

1 Introduction

Accurate dynamic modeling and thrust allocation are essential for underwater vehicle control. Lagrangian or Newton-Euler formulations are commonly

B. Thool
Indian Institute of Technology Mandi, Himachal Pradesh, India
e-mail: S23018@students.iitmandi.ac.in

Jagadeesh Kadiyam
Indian Institute of Technology Mandi, Himachal Pradesh, India
e-mail: jagadeesh@iitmandi.ac.in

S. Mohan
Indian Institute of Technology Palakkad, Kerala, India
e-mail: santhakumar@iitpkd.ac.in

used to describe vehicle dynamics. Lagrangian methods offer systematic derivations; however, their computational complexity escalates significantly with increasing degrees of freedom, thereby constraining their applicability to multibody systems. As a result, Newton-Euler formulations, especially the one proposed by Fossen [3, 4], are the most common in marine robotics and form the basis for most current control and thrust allocation methods. Despite their effectiveness, classical Newton-Euler models rely on Euler-angle transformations, which are difficult to handle in multibody systems because they introduce explicit coupling terms, repeated coordinate transformations, and kinematic singularities. To address these problems, a Denavit-Hartenberg (DH)-based Newton-Euler formulation has been proposed [7]. This formulation gives a compact, modular, and singularity-free dynamic representation for multibody underwater vehicles.

Beyond dynamic modeling, propulsion and thrust allocation are equally critical to underwater vehicle performance. Actuator saturation and hydrodynamic disturbances can reduce propulsion efficiency and vehicle endurance. Consequently, a wide range of thrust allocation methods has been proposed [5]. Early quadratic approaches using pseudoinverse or Lagrange multipliers [12] overlook actuator saturation constraints, leading to diminished performance [1]. Optimization-based and model predictive control (MPC) methods improve realism, albeit at a higher computational expense [10]. Researchers have also examined different actuator configurations, including fixed and vector thrusters [6], energy-efficient configurations [13], and convertible designs [9]. However, increased actuator redundancy complicates thrust distribution. As a result, optimization-based methods, especially quadratic programming, have attracted attention for incorporating energy objectives and actuator constraints [11, 8].

Despite these advances, most thrust allocation methods rely on the classical Fossen-based NewtonEuler framework. The integration of optimization-based allocation with DH-parameter-based dynamics remains limited. This paper presents a unified framework combining DH-based vehicle dynamics with constrained quadratic optimization to handle actuator saturation and hydrodynamic effects for efficient real-time thrust allocation.

The main contributions of this paper are:

- A DH-parameter-based Newton-Euler dynamic formulation that uses virtual frames to represent full six-degree-of-freedom(DOF) underwater vehicle motion and implicitly capture coupling effects.
- The DH-based framework now includes hydrodynamic forces, added mass, damping, and restoring effects, providing a consistent dynamic model for optimization-based thrust allocation.
- A constrained thrust allocation formulation integrates DH-based dynamics with a quadratic programming problem to handle asymmetric thruster saturation and energy-efficient thrust distribution.

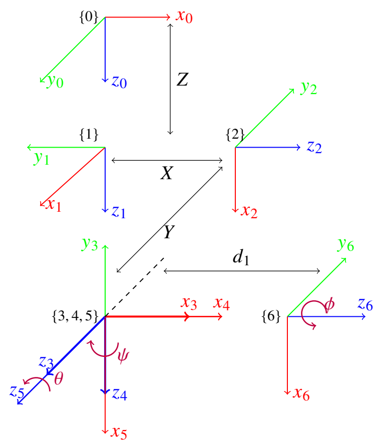

UVMS coordinate frames

D-H Table

Sr.No	α	a	θ	d
1	0	0	$\pi/2$	Z
2	$\pi/2$	0	$\pi/2$	X
3	$\pi/2$	0	$\pi/2$	Y
4	$\pi/2$	0	ψ	0
5	$\frac{3\pi}{2}$	0	$\frac{3\pi}{2}+\theta$	0
6	$\frac{3\pi}{2}$	0	ϕ	d_1

Fig. 1 Coordinate frame transformation using DH parameters for underwater vehicles.

2 Methodology

2.1 DH-based dynamic modeling

While classical 6-DOF formulations provide a complete dynamic description, their reliance on Euler-angle transformations introduces significant trigonometric complexity and kinematic singularities. To address these limitations, a Denavit-Hartenberg (DH) parameter-based virtual frame representation is adopted, in which vehicle motion is modeled as a sequence of DH-parameterized virtual frames, yielding a compact and computationally efficient Newton-Euler formulation.

Unlike conventional DH formulations for manipulators, the virtual frames represent successive inertial-to-body transformations. Starting from the inertial frame, each transformation consists of translations along the Z, X, and Y axes, followed by roll, pitch, and yaw rotations. The resulting transformation chain is summarized in Fig. 1. Using the forward propagation in (1), a kinematic relation is established in which the velocity v_i and acceleration a_i of body i are computed from the motion v_f and a_f of its parent frame $f\{i\}$, augmented by terms induced by the joint motion $\dot{q}_i$ and $\ddot{q}_i$. Here, $\dot{q}_i \in \mathbb{R}$ denotes the scalar rate of the ith virtual joint associated with a single DH transformation. The 6-DOF floating-base motion is realized through a sequence of 6 independent one-DOF virtual joints, such that the stacked velocity vector $\dot{\boldsymbol{q}} = [\dot{q}_1, \ldots, \dot{q}_6]^T \in \mathbb{R}^6$. Accordingly, $\dot{q}_i$ represents a local relative motion between successive frames and should not be interpreted as an element of a single multi-DOF joint velocity. The resulting body acceleration is obtained during the forward pass of the propagation.

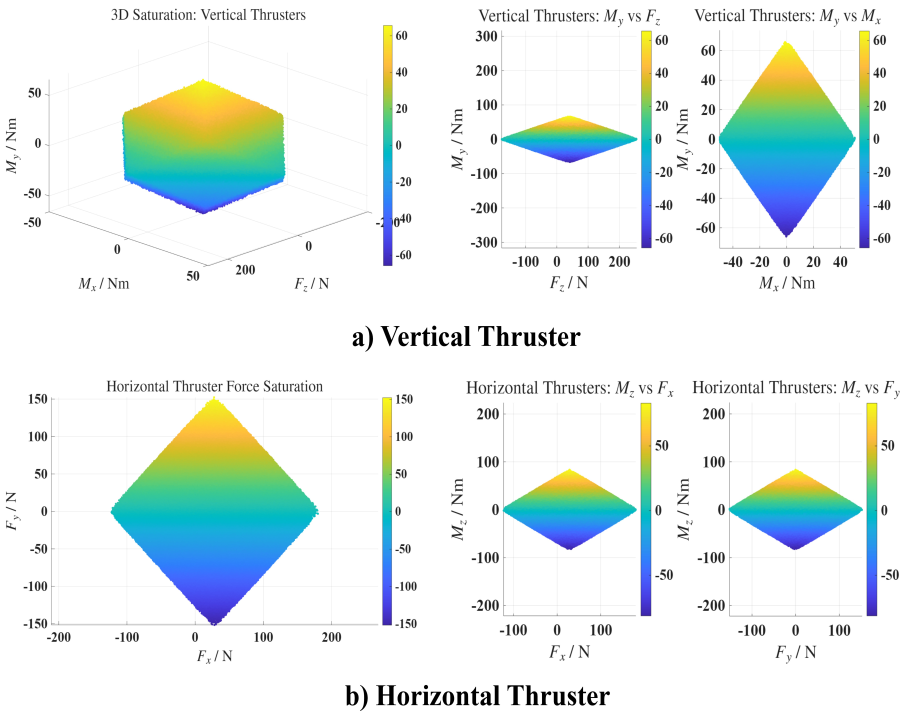

Fig. 2 Thrust saturation envelopes of vertical and horizontal thrusters.

$$
\begin{aligned}
\boldsymbol{\omega}_{i+1} &= \boldsymbol{\omega}_i + [0\ 0\ \dot{q}_{i+1}]^T \\
\boldsymbol{\alpha}_{i+1} &= \boldsymbol{R}_i^{i+1}\left(\boldsymbol{\alpha}_i + \boldsymbol{\omega}_i \times [0\ 0\ \dot{q}_{i+1}]^T\right) + [0\ 0\ \ddot{q}_{i+1}]^T, \\
\boldsymbol{v}_{i+1} &= \boldsymbol{R}_i^{i+1}\left(\boldsymbol{v}_i + \boldsymbol{\omega}_i \times \boldsymbol{P}_i^{i+1}\right) \\
\boldsymbol{a}_{i+1} &= \boldsymbol{R}_i^{i+1}\left(\boldsymbol{a}_i + \boldsymbol{\alpha}_i \times \boldsymbol{P}_i^{i+1} + \boldsymbol{\omega}_i \times (\boldsymbol{\omega}_i \times \boldsymbol{P}_i^{i+1})\right).
\end{aligned}
\tag{1}
$$

where $\boldsymbol{R}_i^{i+1}$ denotes the rotation matrix between successive frames, $\boldsymbol{P}_i^{i+1}$ is the position vector between the origins of frames $\{i\}$ and $\{i+1\}$, and q_i represents the virtual joint variable associated with each DH transformation.

The recursion is initialized with zero angular velocity in the inertial frame as

$$
\boldsymbol{\omega}_0 = \left[0\ 0\ 0\right]^T, \qquad \boldsymbol{\omega}_1 = \boldsymbol{R}_0^1 \boldsymbol{\omega}_0. \tag{2}
$$

Backward recursion accumulates forces and moments across virtual frames to compute the body wrench, preserving dynamic fidelity while reducing computational complexity [7].

Ocean currents represent a dominant environmental disturbance in underwater vehicle (UV) operations and significantly affect vehicle dynamics. In this work, ocean currents are modeled as an external flow field expressed in the inertial (Earth-fixed) frame $\{E\}$, with velocity $\boldsymbol{U}_c^E = \left[u_c^E\ v_c^E\ w_c^E\right]^T$, where u_c^E, v_c^E, and w_c^E denote the surge, sway, and heave components, respectively. The current is assumed to be irrotational, spatially uniform, and slowly varying, which is standard in control-oriented AUV modeling and remains valid over the short prediction horizons considered. Under this assumption, hydrodynamic effects depend on the relative velocity $\boldsymbol{U}_r = \boldsymbol{U} - \boldsymbol{U}_c^E$, where $\boldsymbol{U}$ is the vehicle translational velocity in $\{E\}$. The current direction is parameterized by the angle of attack α and sideslip angle β as

$$u_c^E = U_c \cos\alpha \cos\beta, \quad v_c^E = U_c \sin\beta, \quad w_c^E = U_c \sin\alpha \cos\beta, \tag{3}$$

with U_c denoting the current magnitude. The inertial-frame current velocity is transformed into the body-fixed frame $\{V\}$ using the rotation matrix $\boldsymbol{R}(\boldsymbol{\eta})$ as $\boldsymbol{U}_c^V = \boldsymbol{R}^T(\boldsymbol{\eta})\boldsymbol{U}_c^E$. Accordingly, the relative body-fixed velocity becomes $\boldsymbol{\nu}_r = \boldsymbol{\nu} - \left[\boldsymbol{U}_c^V \ \boldsymbol{0}_{3\times1}\right]^T$, where $\boldsymbol{\nu}$ denotes the vehicle velocity in $\{V\}$.

The relative velocity $\boldsymbol{\nu}_r$ replaces the absolute velocity in the hydrodynamic terms of the NewtonEuler equations, producing a current-aware dynamic model. Variations in flow parameters modify hydrodynamic forces through $\boldsymbol{\nu}_r$ and therefore change the required generalized wrench $\boldsymbol{\tau}$. Because thrust allocation is formulated as a convex optimization problem with bounded actuator inputs, stable thrust distribution is maintained under moderate current disturbances while satisfying actuator constraints.

$$\boldsymbol{M}\dot{\boldsymbol{\nu}} + \boldsymbol{C}(\boldsymbol{\nu}_r)\boldsymbol{\nu}_r + \boldsymbol{D}(\boldsymbol{\nu}_r)\boldsymbol{\nu}_r + \boldsymbol{g}(\boldsymbol{\eta}) = \boldsymbol{\tau}, \tag{4}$$

The generalized wrench $\boldsymbol{\tau}$ obtained from the DH-based NewtonEuler formulation represents the total force and moment required to achieve the desired vehicle motion. This wrench is distributed among individual thrusters through the thrust allocation algorithm described in Section 3, where actuator forces $\boldsymbol{f}$ are computed such that the thrust configuration matrix satisfies $\boldsymbol{K}\boldsymbol{f} = \boldsymbol{\tau}$ while respecting saturation limits. Thus, the DH-based dynamic model provides the required body wrench, and the optimization-based allocator determines feasible thruster commands. Figure 2 illustrates attainable wrench envelopes under asymmetric thruster limits ($f_{\min} = -45$ N, $f_{\max} = 65$ N), showing coupled constraints for vertical thrusters and diamond-shaped feasible regions for horizontal thrusters, highlighting restrictions imposed by actuator limits and environmental disturbances.

3 Thrust allocation based on Quadratic Programming

Quadratic programming formulation:- Actuator saturation, asymmetric thrust limits, and actuation system redundancy inherently constrain thrust allocation in underwater vehicles. These constraints preclude direct inversion of the thrust configuration matrix, motivating the use of an optimization-based allocation approach. Accordingly, thrust allocation is formulated as a quadratic programming (QP) problem, where the objective is to compute an optimal thruster force vector $\boldsymbol{f} \in \mathbb{R}^8$ that minimizes energy consumption while accurately realizing the desired generalized force vector $\boldsymbol{\tau}$.

The fundamental energy-minimization objective is formulated as

$$\min_{\boldsymbol{f}} \ \frac{1}{2}\boldsymbol{f}^T\boldsymbol{H}\boldsymbol{f} \quad \text{s.t.} \quad \boldsymbol{K}\boldsymbol{f} = \boldsymbol{\tau},\ \boldsymbol{f}_{\min} \leq \boldsymbol{f} \leq \boldsymbol{f}_{\max}. \tag{5}$$

where $\boldsymbol{K}$ is the thrust configuration matrix and $\boldsymbol{H} \succ 0$ is a weighting matrix. Since all thrusters have identical characteristics and no failures are assumed, $\boldsymbol{H}$ is chosen as the identity matrix. To explicitly account for thrust saturation and tracking accuracy, the objective is augmented with a penalty on the force tracking error, yielding the following quadratic program:

$$\min_{\boldsymbol{f}} \ \frac{1}{2}\boldsymbol{f}^T\boldsymbol{H}\boldsymbol{f} + \omega \left\|\boldsymbol{K}\boldsymbol{f} - \boldsymbol{\tau}\right\|_2^2 \quad \text{s.t.} \quad \boldsymbol{f}_{\min} \leq \boldsymbol{f} \leq \boldsymbol{f}_{\max}. \tag{6}$$

where $\omega > 0$ is a scalar weighting factor that balances energy minimization and control fidelity.

Optimality and convexity properties:- The thrust allocation problem is a strictly convex quadratic program, since:

- $\boldsymbol{H} \succ 0$ ensures strict convexity of the objective function.
- The equality and box constraints define a closed and convex feasible set.

Under these conditions, the problem admits a unique global optimal solution. Moreover, the Karush-Kuhn-Tucker (KKT) conditions are both necessary and sufficient for optimality, ensuring convergence to the global optimum under standard convexity assumptions [2].

ADMM-Based Solution Without Explicit Active Sets:-To enable efficient real-time implementation, the thrust allocation problem is solved using an Augmented Lagrangian-based ADMM framework, avoiding explicit active-set partitioning. Introducing a slack variable $\boldsymbol{s} \in \mathbb{R}^8$, the box constraints are rewritten as $\boldsymbol{f} - \boldsymbol{s} = \boldsymbol{0}, \qquad \boldsymbol{s} \in [\boldsymbol{f}_{\min}, \boldsymbol{f}_{\max}]^8$. The augmented Lagrangian is then defined as

$$\begin{aligned}\mathcal{L}(\boldsymbol{f}, \boldsymbol{s}, \boldsymbol{\lambda}, \boldsymbol{\mu}) = &\frac{1}{2}\boldsymbol{f}^T\boldsymbol{H}\boldsymbol{f} + \omega\|\boldsymbol{K}\boldsymbol{f} - \boldsymbol{\tau}\|_2^2 + \boldsymbol{\lambda}^T(\boldsymbol{\tau} - \boldsymbol{K}\boldsymbol{f}) \\ &+ \boldsymbol{\mu}^T(\boldsymbol{f} - \boldsymbol{s}) + \frac{\rho_1}{2}\|\boldsymbol{\tau} - \boldsymbol{K}\boldsymbol{f}\|_2^2 + \frac{\rho_2}{2}\|\boldsymbol{f} - \boldsymbol{s}\|_2^2,\end{aligned} \tag{7}$$

where $\boldsymbol{\lambda}$ and $\boldsymbol{\mu}$ are Lagrange multipliers and $\rho_1, \rho_2 > 0$ are penalty parameters.

The ADMM iterations consist of the following steps:

1) Primal variable update

The thruster force vector $\boldsymbol{f}$ is updated in closed form by solving a linear system,

$$\boldsymbol{f}^{k+1} = \boldsymbol{Q}^{-1}\boldsymbol{q}, \tag{8}$$

$$\boldsymbol{Q} = \boldsymbol{H} + (2\omega + \rho_1)\boldsymbol{K}^T\boldsymbol{K} + \rho_2\boldsymbol{I}, \qquad \boldsymbol{q} = (2\omega + \rho_1)\boldsymbol{K}^T\boldsymbol{\tau} + \boldsymbol{K}^T\boldsymbol{\lambda}^k - \boldsymbol{\mu}^k + \rho_2\boldsymbol{s}^k. \tag{9}$$

2) Slack variable update

The slack variable $\boldsymbol{s}$ is updated via projection onto the admissible box constraints,

$$\boldsymbol{s}^{k+1} = \mathcal{P}_{[\boldsymbol{f}_{\min}, \boldsymbol{f}_{\max}]}\left(\boldsymbol{f}^{k+1} + \frac{1}{\rho_2}\boldsymbol{\mu}^k\right). \tag{10}$$

3) Dual variable updates

The Lagrange multipliers are updated as

$$\boldsymbol{\lambda}^{k+1} = \boldsymbol{\lambda}^k + \rho_1(\boldsymbol{\tau} - \boldsymbol{K}\boldsymbol{f}^{k+1}), \qquad \boldsymbol{\mu}^{k+1} = \boldsymbol{\mu}^k + \rho_2(\boldsymbol{f}^{k+1} - \boldsymbol{s}^{k+1}). \tag{11}$$

Under standard ADMM convergence conditions, the iterates converge to the unique global optimum of the thrust allocation problem. The closed-form updates enable computationally efficient implementation. In this study, penalty parameters were selected empirically as $\rho_1 = 1$ and $\rho_2 = 5$, which ensured stable convergence in all simulations. Iterations were terminated when $\|\boldsymbol{f}^{k+1} - \boldsymbol{f}^k\|_2/\|\boldsymbol{f}^k\|_2 < 10^{-4}$ or after 20 iterations. Convergence typically occurred within 8-12 iterations per control step, supporting real-time applicability. The computational cost is dominated by solving the linear system in (8); since $\boldsymbol{Q}$ is constant, its factorization can be precomputed offline, reducing to matrix-vector operations.

4 Results and Discussion

This section evaluates the proposed ADMM-based quadratic programming (QP) thrust allocation through simulations using vehicle and hydrodynamic parameters from [6]. Circular trajectories with and without ocean currents are considered, and performance is compared with pseudoinverse (least-squares) allocation.

Circular trajectory tracking without ocean current:- For 3D circular motion, both the pseudoinverse (LS) and ADMM-based QP methods achieve stable tracking, as shown in Fig. 3(a). The ADMM-based allocator follows the reference trajectory more closely, particularly along curved segments. Thruster force histories in Fig. 3(b) show larger transients and oscillations for the LS method, while the QP-based approach produces smoother thrust profiles. Consequently, Fig. 3(c,d) indicates moderate reductions in per-thruster and total energy consumption with the ADMM-based allocation.

Circular trajectory tracking with ocean current disturbance:- Under steady ocean currents, Fig. 4(a) shows that the ADMM-based allocator main-

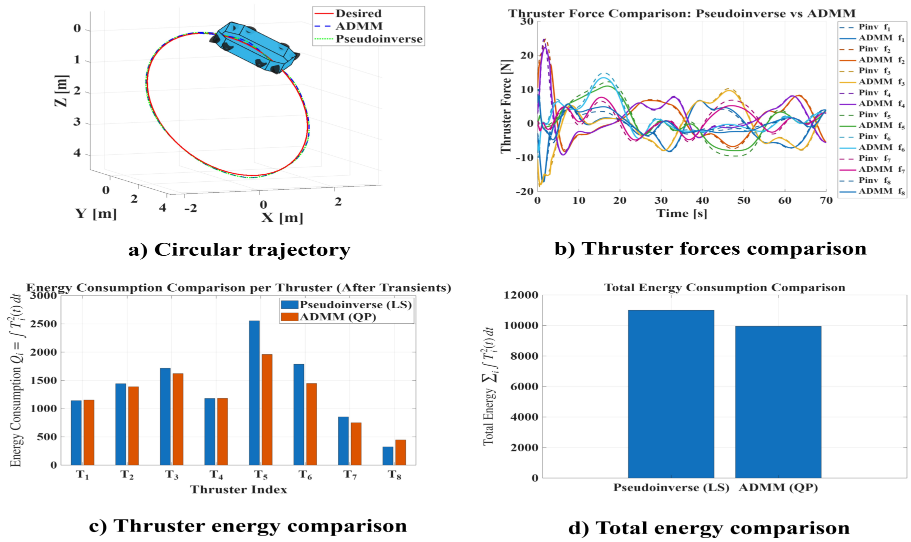

Fig. 3 Compared with pseudoinverse allocation, the ADMM-based QP method achieves closer circular trajectory tracking (a), smoother and lower-amplitude thruster forces (b), reduced per-thruster energy consumption (c), and significantly lower total propulsion energy (d), demonstrating improved efficiency and constraint handling.

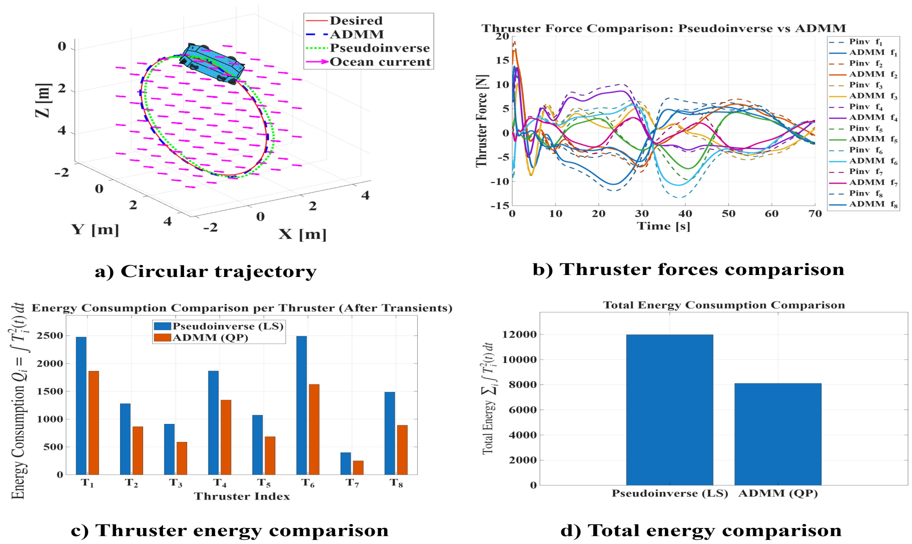

Fig. 4 Under steady ocean currents, the ADMM-based allocator achieves closer circular trajectory tracking (a), smoother thruster force profiles (b), reduced per-thruster energy usage (c), and lower total propulsion energy (d) compared to the pseudoinverse method.

tains closer tracking than the pseudoinverse method, which exhibits larger deviations. Thruster force histories in Fig. 4(b) reveal increased oscillations and thrust reversals for the LS approach, while the QP-based method produces smooth, bounded commands. Consequently, Fig. 4(c,d) demonstrates substantial reductions in both per-thruster and total energy consumption with the ADMM-based allocation, highlighting its robustness under environmental disturbances.
Although the evaluation is based on simulation, the adopted hydrodynamic parameters and disturbance models are representative of practical underwater vehicles and allow meaningful comparison between thrust allocation strategies.

5 Conclusion

This paper introduced ADMM-based quadratic programming for constrained thrust allocation in over-actuated underwater vehicles. In simulations with complex trajectories and ocean currents, the method achieves smoother thrust profiles, improved trajectory tracking, and reduced energy consumption by accounting for asymmetric thruster saturation and energy minimization. Vehicle dynamics are modeled using a DH-parameter-based NewtonEuler formulation, which simplifies equation derivation while preserving dynamic accuracy. Future work will include the development of interaction-aware thruster models and efficiency maps, along with validation using higher-fidelity hydrodynamic simulations and experimental testing with a physical underwater vehicle platform.

References

1. Arditti, F., Souza, F.L.d., Martins, T.d.C., Tannuri, E.A.: Thrust allocation algorithm with efficiency function dependent on the azimuth angle of the actuators. Ocean Engineering **105**, 206–216 (2015)
2. Deng, L., Tao, J.: Thrust allocation control of an underwater vehicle with a redundant thruster configuration. Mathematics **13**(11), 1766 (2025)
3. Fossen, T.I.: Guidance and control of ocean vehicles. Wiley (1994)
4. Fossen, T.I.: Handbook of marine craft hydrodynamics and motion control. John Willy & Sons Ltd (2011)
5. Johansen, T.A., Fossen, T.I.: Control allocationa survey. Automatica **49**(5), 1087–1103 (2013)
6. Kadiyam, J., Mohan, S., Deshmukh, D., Seo, T.: Simulation-based semi-empirical comparative study of fixed and vectored thruster configurations for an underwater vehicle. Ocean Engineering **234**, 109231 (2021)
7. Krishnan, K.A., Kadiyam, J., Mohan, S.: Underwater vehicle modelling with newton-euler method using dh parameters. In: ISOPE Pacific/Asia Offshore Mechanics Symposium, pp. ISOPE–P. ISOPE (2024)

8. Rethfeldt, C., Jeinsch, T.: Combined actuator allocation for underwater vehicles with variable buoyancy systems using qp-based optimization. In: OCEANS 2024-Halifax, pp. 1–7. IEEE (2024)
9. Tanakitkorn, K., Phoemsapthawee, S.: Impacts of thruster configurations on the task performance of an unmanned surface vehicle. Ocean Engineering **256**, 111465 (2022)
10. Veksler, A., Johansen, T.A., Borrelli, F., Realfsen, B.: Dynamic positioning with model predictive control. IEEE Transactions on Control Systems Technology **24**(4), 1340–1353 (2016)
11. Wang, Y., Huang, Y., Li, Y., Ren, C.: Optimization of thruster configuration and control allocation for a spherical magnetic coupling thrusters actuated underwater robot. Ocean Engineering **309**, 118445 (2024)
12. Wei, Y., Fu, M., Ning, J., Sun, X.: Quadratic programming thrust allocation and management for dynamic positioning ships. TELKOMNIKA Indonesian Journal of Electrical Engineering **11**(3), 1632–1638 (2013)
13. Xu, D., Yan, Z., Xie, H., Lu, L., Xiao, Z., Han, B.: Demand-driven optimization method for thruster configuration of underwater vehicles considering capability boundary and system efficiency. Ocean Engineering **310**, 118749 (2024)